

Characterization of normal and inverted interfaces by the Zeeman effect in $\text{Cd}_{1-x}\text{Mn}_x\text{Te}/\text{CdTe}/\text{Cd}_{1-y}\text{Mg}_y\text{Te}$ quantum wells

A. Lemaître, C. Testelin, and C. Rigaux

Groupe de Physique des Solides, Universités Paris 6 et 7, 2 place Jussieu, 75231 Paris Cedex 05, France

S. Maćkowski, Nguyen The Khoi, and J. A. Gaj

Institute of Experimental Physics, Warsaw University, 69 Hoża, 00-681 Warszawa, Poland

G. Karczewski, T. Wojtowicz, and J. Kossut

Institute of Physics, Polish Academy of Sciences, Aleja, Lotników 32/46, Warszawa, Poland

(Received 13 May 1997; revised manuscript received 10 October 1997)

We present a study of the interface profile in asymmetric $\text{Cd}_{1-x}\text{Mn}_x\text{Te}/\text{CdTe}/\text{Cd}_{1-y}\text{Mg}_y\text{Te}$ quantum wells, with normal ($\text{Cd}_{1-x}\text{Mn}_x\text{Te}$ on CdTe) and inverted (CdTe on $\text{Cd}_{1-x}\text{Mn}_x\text{Te}$) interfaces. The Zeeman spectra of the confined exciton states were determined by magnetorefectivity and Kerr rotation measurements. Using a segregation model and an asymmetric exponential profile, we interpret the Zeeman spectra of quantum wells, and determine the interface widths. For the same concentrations of Mn in the barriers and the same growth conditions, the results can be coherently explained assuming an interface width independent of the quantum-well width and the type of interface (normal or inverted). [S0163-1829(98)04607-4]

I. INTRODUCTION

Characterization of interfaces by means of Zeeman effect measurements has been shown to be an efficient tool to determine the interface mixing between adjacent CdTe and $\text{Cd}_{1-x}\text{Mn}_x\text{Te}$ layers in molecular-beam-epitaxy-grown quantum wells and superlattices.¹ The Zeeman effect characterization method (called also spin tracing) also allows one to check whether the quantum-well profiles are symmetric or not. In particular, it has been shown that the Zeeman effect in quantum wells containing manganese in one of the barriers only changes by as much as a factor of 4 depending on the growth order of such quantum wells: exciton levels in quantum wells with inverted (CdTe grown on $\text{Cd}_{1-x}\text{Mn}_x\text{Te}$) interfaces split in a magnetic field much stronger than those in quantum wells with normal ($\text{Cd}_{1-x}\text{Mn}_x\text{Te}$ on CdTe) interfaces.^{1,2} This effect has been explained as resulting from an exchange of atoms between two adjacent layers during growth,³ producing exponential-like, strongly asymmetric interface profiles. Such a mechanism has been discussed previously for III-V compounds⁴ and is known as segregation mechanism of interface mixing. The above-mentioned ideas have been tested on ten samples, grown at the Centre National de la Recherche Scientifique—Commissariat à l’Energie Atomique (CNRS-CEA) group in Grenoble containing quantum wells of similar width (around 15 ML) with the barriers of $\text{Cd}_{1-y}\text{Zn}_y\text{Te}$ (~ 13 at. % Zn) and $\text{Cd}_{1-x}\text{Mn}_x\text{Te}$ (~ 35 at. % Mn).

A qualitatively different behavior has been reported in Ref. 5 for smaller quantum-well width values. While confirming the above-mentioned regularity for relatively wide quantum wells (60 Å), for a pair of wells 24 Å wide the authors measured identical Zeeman splittings for the normal and inverted interfaces, whereas for a well width of 12 Å they reported a much stronger Zeeman splitting in case of the

normal interface. Their results seem to be incompatible with the idea of the segregation mechanism. The results of Ref. 5 were obtained on three pairs of quantum wells of thickness 60-, 24-, and 12-Å widths, respectively, with the barriers of $\text{Cd}_{1-x}\text{Mn}_x\text{Te}$ and $\text{Cd}_{1-y}\text{Mg}_y\text{Te}$ of about 22% of Mn and Mg.

In this work we performed Zeeman effect measurements on a series of asymmetric $\text{Cd}_{1-x}\text{Mn}_x\text{Te}/\text{CdTe}/\text{Cd}_{1-y}\text{Mg}_y\text{Te}$ quantum wells in a continued effort to understand the properties of normal and inverted interfaces in $\text{CdTe}/\text{Cd}_{1-x}\text{Mn}_x\text{Te}$ system.

II. SAMPLES AND EXPERIMENTS

The samples were grown by molecular beam epitaxy (MBE) in the Institute of Physics of the Polish Academy of Sciences in Warsaw. The samples were grown on (100)-oriented GaAs substrates with a 3–4- μm -thick CdTe buffer layer. The substrate temperature during the growth was approximately 280 °C. We studied two pairs of samples each containing three uncoupled CdTe quantum wells QW_1 , QW_2 , and QW_3 of different widths (15, 11, and 8 ML, respectively) surrounded by thick $\text{Cd}_{1-x}\text{Mn}_x\text{Te}$ and $\text{Cd}_{1-x}\text{Mg}_x\text{Te}$ barrier layers. For both samples (*A* and *B*) forming the pair, the nominal parameters, such as the well width and the composition of the barrier materials, are nominally identical. Samples *A* and *B* differ only by the growth sequence, as indicated in Fig. 1. The semimagnetic interfaces of QW_1 , QW_2 , and QW_3 are either normal ($\text{Cd}_{1-x}\text{Mn}_x\text{Te}$ on CdTe) or inverted (CdTe on $\text{Cd}_{1-x}\text{Mn}_x\text{Te}$) depending on the type of structure. The actual parameters of the samples are given in Table I. Two pairs (11 206 and 04 296) with different composition of the barrier materials and identical well width L_1 , L_2 , and L_3 were investigated. An additional sample 06 126*B*, displaying a structure of type *B*, with an intermediate Mn composition, was also studied.

Energies of heavy-hole ground state E_1H_1 quantum-well excitons in a magnetic field were determined by magnetore-

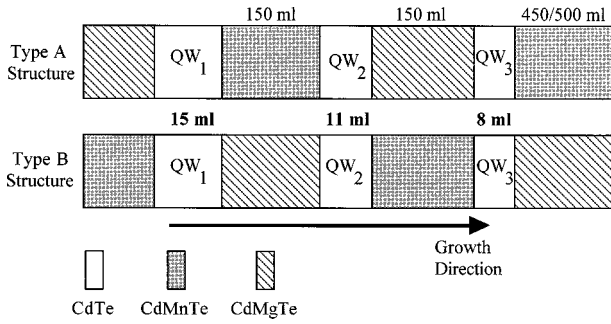


FIG. 1. Sequence of layers in the investigated samples of types A and B, having semimagnetic barriers at the normal or the inverted interface (substrates and buffers omitted for clarity).

flectivity experiments performed in the Faraday geometry with circularly polarized radiation (σ^\pm). The measurements were made at near-normal incidence on samples immersed in superfluid helium at 1.7 K, in the presence of a magnetic field ($H \leq 5$ T) applied along the growth axis. The polar magneto-optic Kerr effect (MOKE) was also used in addition to magnetorefectance experiments to determine precisely the energies of the Zeeman components of the QW exciton transitions. This technique as described in Ref. 6 is particularly suitable to extract magneto-optical transition energies from the reflectivity spectra in the case of strong influence by interferences of light in these multilayer structures. The transition energies were determined from precise fits (Ref. 6), allowing us to reproduce the observed line shapes. Figure 2 shows examples of such fits done for two structures exhibiting different shapes.

Because of uncertainty of the position of the exciton transition in the reflectivity spectrum, the photoluminescence excitation (PLE) experiments turned out to be necessary in the case of QW₃ in sample 11 206B. PLE spectra were taken using a COHERENT CR-599 tunable dye laser working with

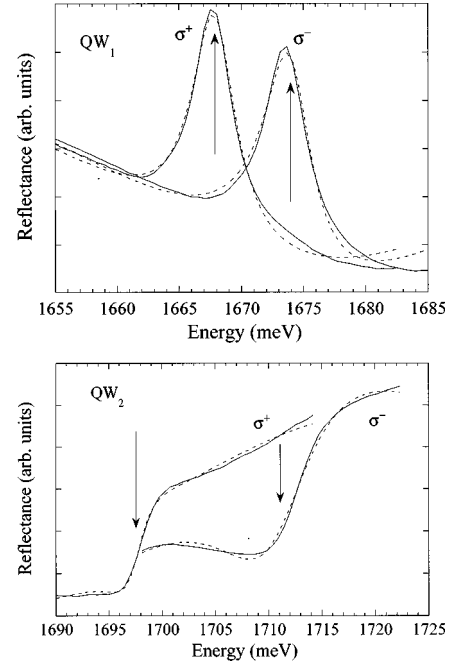


FIG. 2. Experimental (solid) and calculated (dashed) reflectivity spectra of the excitonic structures corresponding to quantum wells QW₁ and QW₂ (nominal widths of 15 and 11 ML respectively) of sample 04296A. Temperature 1.6 K, magnetic field 2 T. Excitonic energies are determined from the fits indicated by arrows.

4-dicyanomethylene-2-methyl-6-(p-dimethylamino)styryl)-4H-pyran (DCM), and pumped by a 5-W light beam of an INNOVA-70 Ar laser. The linearly polarized exciting laser beam of about 20 mW was transformed by a PEM-80 photoelastic modulator into alternating left- and right-circularly polarized beams, and focused onto a spot with the diameter of 1 mm on the sample. The luminescence light coming out from the sample was collected on an entrance slit of a mono-

TABLE I. Parameters of the samples. Labels A or B indicate the sample type (see Fig. 1). Labels N and I indicate the Cd_{1-x}Mn_xTe/CdTe interface type, normal (N) or inverted (I).

Sample	Barrier composition		QW width (monolayers)		Cd _{1-x} Mn _x Te/CdTe interface	Zero field Energy (meV)	Zeeman splitting at 5 T (meV)	Intermixing length (Å)
	Mn(%)	Mg(%)	Nominal	Adjusted				
11 206A	47.2	47.2	15	14.9	N	1702.4	1.6	3.5±0.3
			11	11	I	1766.3	15.6	3.8±0.3
			8	7.7	N	1856.3	7.0	2.9±0.5
11 206B	47.2	47.2	15	13.7	I	1716.9	8.9	3.5±0.2
			11	10.1	N	1782.3	3.9	3.1±0.3
			8	7.5	I	1870.8	22.6	3.4±0.4
04 296A	13.9	24.6	15	14.89	N	1671.2	9.1	4.5±0.4
			11	10.78	I	1706.4	22.4	4.5±0.4
			8	7.99	N	1744.3	32.8	5.5±0.5
04 296B	14.9	26.8	15	13.91	I	1680.9	14.55	4.7±0.4
			11	10.3	N	1722.8	22.15	5.7±0.5
			8	7.68	I	1758.6	42.1	5.5±0.5
06 126B	31.3	26	15	12.74	I	1709.7	12.9	4.3±0.3
			11	9.2	N	1762.8	8.3	3.7±0.5
			8	6.79	I	1825.9	30.9	4.5±0.3

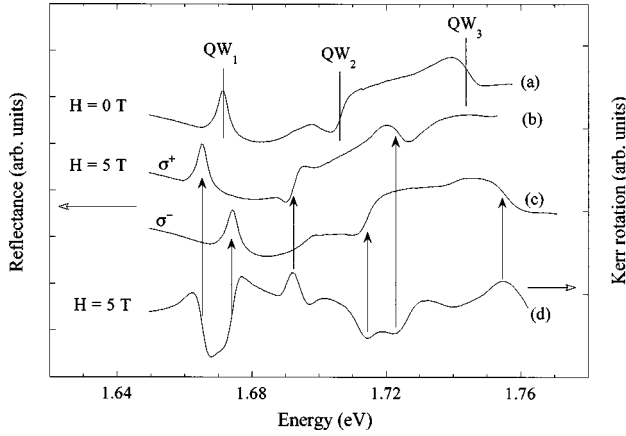


FIG. 3. Zero-field reflectivity spectrum of sample 04 296A at $T=1.7$ K (curve *a*): the vertical lines indicate the positions of the QW_1 , QW_2 , and QW_3 exciton structures displaying different line shapes. Comparison of the magnetorefectance spectra at $H=5$ T for σ^+ (curve *b*), and σ^- (curve *c*) polarizations, and the Kerr rotation (curve *d*). The arrows indicate the corresponding positions of the Zeeman components.

chromator adjusted to a photon energy corresponding to the low-energy side of the peak of the luminescence from the considered quantum well. The signal from the photomultiplier was analyzed by a SR-400 two-channel photon counter. Magnetic fields up to $B=5$ T were applied in the Faraday configuration.

III. EXPERIMENTAL RESULTS

The zero-field energy of the QW exciton ground states and of the exciton states in the barriers was determined from the position of corresponding reflectivity features for each sample. The results are collected in Table I. MOKE measurements are particularly useful, since they help to distinguish the exciton structures associated with $Cd_{1-x}Mn_xTe$ and $Cd_{1-x}Mg_xTe$ barriers.

Figure 3 shows an example of the magnetorefectivity and Kerr rotation spectra (at $H=5$ T) for sample 04 296A. The zero-field exciton structures associated with QW_1 , QW_2 , QW_3 are indicated in the reflectivity spectrum. The Zeeman splittings (up to 5 T) of excitons confined in QW's were determined from correlated Kerr and magnetorefectivity measurements (and from PLE in the case of QW_3 in the sample 11 206B) as functions of magnetic field up to 5 T. Figures 4 and 5 show the Zeeman shifts of the σ^+ and σ^- components versus the magnetic field for all three quantum wells QW_1 , QW_2 , and QW_3 of the pairs of samples 11 206 and 04 296, respectively.

A pronounced difference in the Zeeman splitting is visible between the normal and inverted interfaces, especially in samples from the 11 206 series. Because the pairs of the quantum wells with nominally identical thickness differ slightly in their zero-field exciton energies, due to small difference in the well widths, related to small unintentional changes of the growth rate, an alternative way of presentation of the Zeeman effect was chosen in Fig. 6: the Zeeman splitting at 5 T is plotted as a function of the zero-field energy for samples 11 206A and 11 206B. The splitting for the

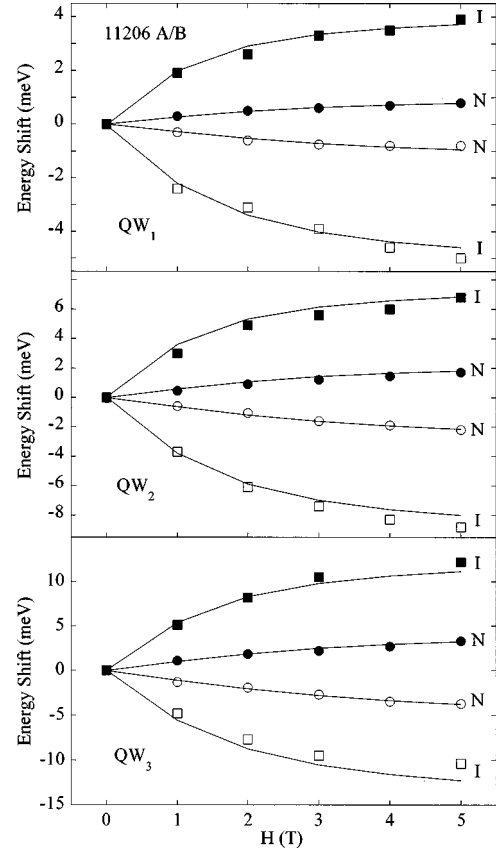


FIG. 4. Zeeman shifts of the heavy-hole exciton ground states confined in QW_1 , QW_2 , and QW_3 quantum wells for samples A and B (series 11 206). Black (σ^-) and open (σ^+) symbols are experimental data obtained for normal (N, circles) and inverted (I, squares) interfaces. Continuous lines are calculated for an asymmetric QW profile for the intermixing lengths ℓ_{Mn} , and the well widths reported in Table I.

inverted interfaces is much greater than that for the normal ones for all the quantum wells, in contrast with the results of Ref. 5 where at a well width of 24 \AA (7.4 monolayers) the splittings for the normal and inverted interfaces are almost identical.

Figure 7 shows similar results for the pair of samples 04 296A and 04 296B, having much smaller Mn mole fraction in barriers than in 11 206 series (about 14–15%). The difference between the normal and inverted interfaces is much smaller here, reflecting a smaller sensitivity of the Zeeman effect to the intermixing in quantum wells with barriers containing less manganese. Taking into account this smaller sensitivity, we can only say that the narrow wells in this pair of samples display similar interface characteristics to those of the wide quantum wells.¹

In summary, we can draw the following conclusion for both pairs of samples discussed so far. There is a qualitative difference between our results and those of Ref. 5, where the Zeeman splittings measured on quantum wells with different interface types, strongly different for wide (60 \AA) wells, become equal for the well width of 24 \AA (7.4 ML). This experimental difference can possibly originate from different MBE growth regimes in the two cases. To produce a quan-

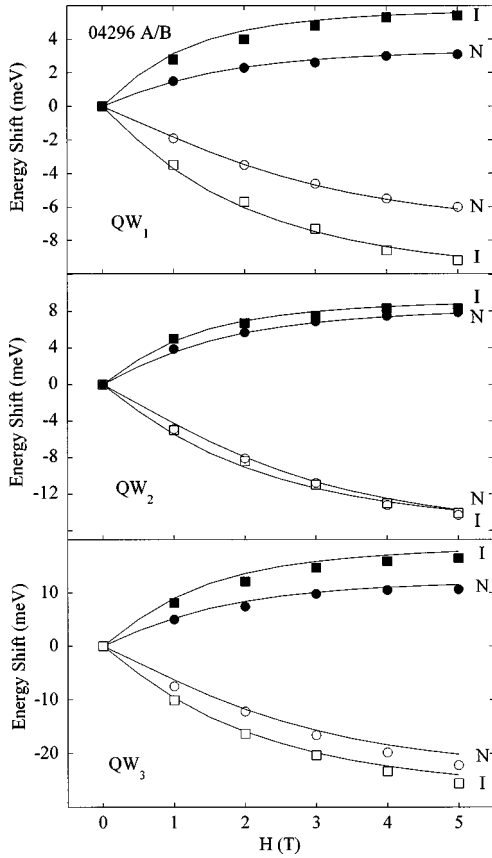


FIG. 5. Same as Fig. 4, for samples A and B (series 04 296).

titative interpretation we perform simulations of excitonic states in quantum wells.

IV. INTERFACE MIXING MODEL AND DISCUSSION

The Zeeman effect in normal and inverted $\text{Cd}_{1-x}\text{Mn}_x\text{Te}/\text{CdTe}/\text{Cd}_{1-y}\text{Zn}_y\text{Te}$ quantum wells was measured and explained in terms of a segregation mechanism of the interface mixing,¹⁻³ taking into account the intrinsic and extrinsic effects. In this model, we considered an asymmetric QW profile with an exponential distribution of manganese

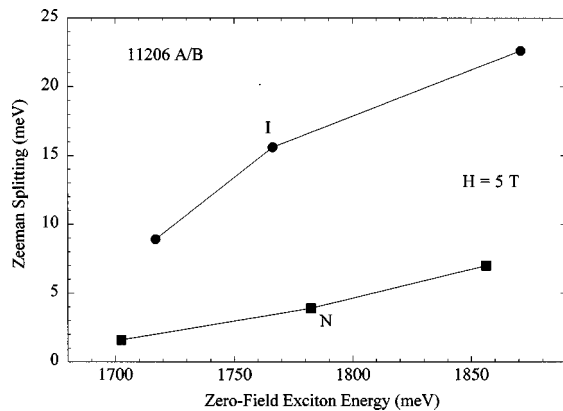


FIG. 6. Zeeman splittings of heavy-hole excitons confined in quantum wells in samples 11 206A and B, at 5 T, plotted as a function of the zero-field exciton energy (given in Table I). Circles and squares are for normal and inverted interfaces, respectively. The lines are to guide the eyes.

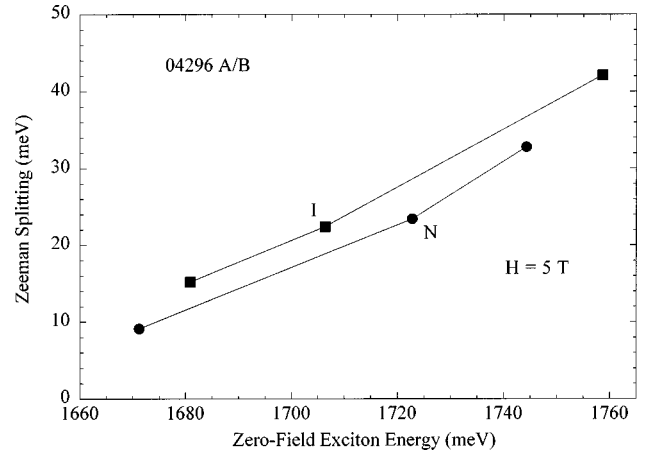


FIG. 7. Same as Fig. 6 for samples 04 296A and 04 296B.

and magnesium ions (ℓ_{Mn} and ℓ_{Mg} are the intermixing lengths of manganese and magnesium, respectively). We used the bulk parameters given in Ref. 3 to estimate the effective spin and the effective temperature of the manganese ions along the profile. The heavy hole and electron-confined states were calculated using a relative valence-band offset $\alpha=0.3$ (results were almost insensitive to the choice of this parameter in the commonly admitted range $\alpha=0.2-0.4$). For the electron effective mass and parallel and perpendicular heavy hole masses, we chose $m_e/m_0=0.099$, $m_{\text{hh}\parallel}/m_0=0.513$, and $m_{\text{hh}\perp}/m_0=0.193$, respectively⁷ (m_0 is the free-electron mass). In order to determine the exciton E_1H_1 level, we calculated the exciton binding energy by using the method developed by Leavitt and Little⁸ and Peyla *et al.*,⁹ with a dielectric constant $\epsilon=10$ (in agreement with the parameters given in Ref. 7).

Despite a calibration of the growth rate by reflection high-energy electron-diffraction oscillations, the real QW width L can differ slightly from its nominal value. Therefore, there are three parameters that we treat as adjustable in our calculation: the QW width and the intermixing lengths ℓ_{Mn} and ℓ_{Mg} . We decided to keep $\ell_{\text{Mn}}=\ell_{\text{Mg}}$ and the QW width was adjusted to reproduce the experimental E_1H_1 transition energy in the absence of the field. There is no apparent reason to have the same intermixing lengths for manganese and magnesium, but we found that the choice of ℓ_{Mg} has a negligible influence on the final results: a change in the magnesium intermixing length will induce a small variation of the zero field energy, easy to compensate by adjusting the QW width L (by less than 1 Å) and a negligible change of the Zeeman splitting. Then the Mn intermixing length is adjusted to reproduce the QW Zeeman spectrum.

Experimental and theoretical Zeeman splittings are presented in the Figs. 4 and 5, for both pairs of samples 11 206 and 04 296. The parameters deduced from this analysis are presented in Table I, for all 15 wells in the five samples studied. An important result is the common value of ℓ_{Mn} for normal and inverted wells on the same sample, and also in the same series (11 206 or 04 296). The samples belonging to three separate series may have been synthesized under slightly different growth conditions. This explains the different values of ℓ_{Mn} in Table I (about 4.8–5.3 Å for 04 296A/B, 4.2 Å for 06 126A, and 3.3–3.4 Å for 11 206A/B). We should also mention that the intermixing

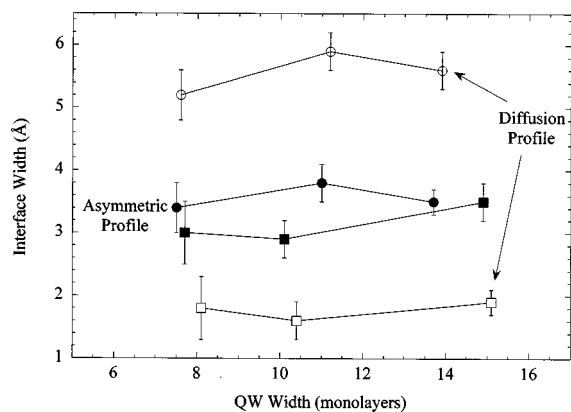


FIG. 8. Interface width vs the quantum-well width for the samples 11 206. Circles and squares are for inverted and normal interfaces, respectively.

length values obtained for the 04 296 series have a much smaller precision because of the small sensitivity of Zeeman splittings to the interface width in the case of magnetically dilute barriers.¹ For the same Mn and Mg concentrations and identical growth conditions, \mathcal{L}_{Mn} is identical for all the QW's within the series.

In order to present clearly the difference between the segregation model used so far and a simple diffusion model, we also performed simulations for a symmetric interface profile (given by the error function as defined in Ref. 1). Figure 8 shows a comparison of the results obtained for the samples from the 11 206 series using both models. While for the asymmetric exponential profiles we obtain very close values of the interface width for both the normal and inverted interfaces (3.2 ± 0.3 and 3.6 ± 0.3 Å, respectively), a symmetric error function profile yields an important difference between the widths of the normal and the inverted interfaces (≈ 1.8

and ≈ 5.6 Å, respectively). In all cases the interface width does not vary significantly with the QW width (the values given above are averaged over the well width). To introduce a physical interpretation of the important difference between the widths of the two types of interface obtained using the simple diffusion model, we may think of a short-range roughness developing during the growth of the $\text{Cd}_{1-x}\text{Mn}_x\text{Te}$ barriers. Such an effect was reported by Jouneau *et al.*¹⁰ for CdTe wells with MnTe barriers. However, comparing samples with $\text{Cd}_{1-x}\text{Mn}_x\text{Te}$ barriers of different thickness, Grieshaber *et al.*³ described all the results with similar accuracy using a segregation model which did not contain such a barrier-thickness-dependent mechanism. Therefore, we think that while a roughness developing with the barrier thickness occurs in nonequilibrium MnTe layers, such a phenomenon is less probable in our case of $\text{Cd}_{1-x}\text{Mn}_x\text{Te}$ barriers with a Mn mole fraction far from 1. It must be pointed out here that we mean only a roughness on the scale of the atomic distances, since only a short-range roughness can be detected by the Zeeman effect, sensitive to changes of the neighborhood of Mn ions.¹

Summarizing the information from all the available sources, we cannot exclude a possibility of an increase of the interface width (roughness) as a result of an inferior growth quality of ternary $\text{Cd}_{1-x}\text{Mn}_x\text{Te}$ or $\text{Cd}_{1-y}\text{Mg}_y\text{Te}$, as compared to the binary CdTe. However, all the results, obtained so far on samples grown by MBE in Grenoble and in Warsaw, can be coherently interpreted within the segregation model using a *single* interface width value for both the normal and inverted interfaces.

ACKNOWLEDGMENT

This work was partially supported by the State Committee for Scientific Research (Poland) under Grant No. 8T11B-014-11.

¹J. A. Gaj, W. Grieshaber, C. Bodin-Deshayes, J. Cibert, G. Feuillet, Y. Merle d'Aubigné, and A. Wasiela, *Phys. Rev. B* **50**, 5512 (1994).

²W. Grieshaber, J. Cibert, J. A. Gaj, Y. Merle d'Aubigné, and A. Wasiela, *Phys. Rev. B* **50**, 2011 (1994).

³W. Grieshaber, A. Haury, J. Cibert, Y. Merle d'Aubigné, A. Wasiela, and J. A. Gaj, *Phys. Rev. B* **53**, 4891 (1996).

⁴J. Moison, C. Guille, F. Houzay, F. Barthe, and M. Van Rompay, *Phys. Rev. B* **40**, 6149 (1989).

⁵G. Schmidt, B. Kuhn-Heinrich, U. Zehnder, W. Ossau, T. Litz, A.

Waag, and G. Landwehr, *Acta Phys. Pol. A* **88**, 897 (1995).

⁶C. Testelin, C. Rigaux, and J. Cibert, *Phys. Rev. B* **55**, 2360 (1997).

⁷C. Neumann, A. Nöthe, and N. Lipari, *Phys. Rev. B* **37**, 922 (1988).

⁸R. Leavitt and J. Little, *Phys. Rev. B* **42**, 11 774 (1990).

⁹P. Peyla, R. Romestain, Y. Merle d'Aubigné, G. Fishman, A. Wasiela, and H. Mariette, *Phys. Rev. B* **52**, 12 026 (1995).

¹⁰P. H. Jouneau, A. Tardot, G. Feuillet, H. Mariette, and J. Cibert, *J. Appl. Phys.* **75**, 7310 (1994).